

# Active Variable Stiffness Fibers for Multifunctional Robotic Fabrics

Michelle C. Yuen, R. Adam Bilodeau, and Rebecca K. Kramer

**Abstract**—In this letter, we introduce active variable stiffness fibers that are made from shape memory alloy and thermally responsive polymers. This combines the actuation of shape memory alloy with the variable stiffness of a thermoplastic using electric current as the stimulus. By combining both actuation and variable stiffness functions, the multifunctional fibers can move to a new position then hold that position without requiring additional power. We explore the possibility of tuning the fibers to meet varying structural and performance demands by selecting different thermoplastics with different glass transition temperatures. Finally, we integrate the active variable stiffness fibers into a fabric to demonstrate multifunctional robotic fabrics that can control the motion of soft, compliant bodies from their surface.

**Index Terms**—Soft material robotics, novel actuators for natural machine motion, flexible robots.

## I. INTRODUCTION

THE emerging field of soft robotics aims to bring highly deformable electromechanical systems for applications in wearables, search-and-rescue, medical devices, exploratory robots, and more. This field actively pushes forward non-conventional actuators, sensors, and structures while removing the frames, motors, and linkages associated with traditional robots. To achieve versatility in soft robotic design, we envision robotic fabrics bringing actuation, sensing, and stiffness control to the exterior of integrated systems. Robotic fabrics are 2D fabrics that can wrap around any highly deformable 3D object (e.g. an inflatable balloon or foam) to create a soft robot. These fabrics are currently expanding the possibilities of wearable and conformable robotics by adding function to textiles and manipulating soft-bodied objects [1]–[3]. With no fixed shape of their own, robotic fabrics can exist on the surface of deformable objects and in spaces that do not have a pre-defined geometry or volume.

In this letter, we introduce active variable stiffness fibers (AVS fibers) made from a combination of shape memory alloy and thermally responsive polymers (e.g. thermoplastics). This combination couples the actuation of shape memory alloy with

Manuscript received August 31, 2015; accepted January 3, 2016. Date of publication January 19, 2016; date of current version February 29, 2016. This paper was recommended for publication by Associate Editor X. Liu and Editor Y. Sun upon evaluation of the reviewers' comments. This work was supported by an Early Career Faculty Grant NNX14A052G from National Aeronautics and Space Administration's Space Technology Research Grants Program. The work of M. C. Yuen was supported by the National Science Foundation Graduate Research Fellowship under Grant DGE-1333468. M. C. Yuen and R. A. Bilodeau are co-first authors.

The authors are with the School of Mechanical Engineering, Purdue University, West Lafayette, IN 47907 USA (e-mail: yuenm@purdue.edu; rbilodea@purdue.edu; rebeccakramer@purdue.edu).

Digital Object Identifier 10.1109/LRA.2016.2519609

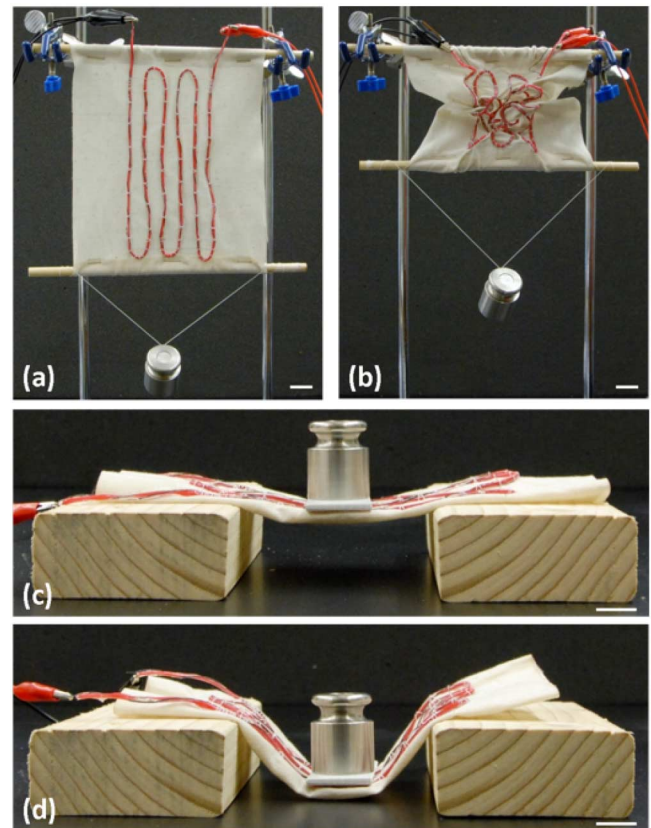


Fig. 1. Active variable stiffness fabric composed of active variable stiffness fibers sewn onto inextensible muslin fabric. (a) Unactuated, stiff AVS fabric with a hanging 200 g mass. (b) Actuated then stiffened AVS fabric holding a 200 g mass. (c) Unactuated, stiff AVS fabric acting as a bridge supporting a 200 g mass on a small plate. (d) Unactuated, softened AVS fabric sinking under the weight of a 200 g mass. Scale bars are 2 cm.

the passive softening/holding capabilities (variable stiffness) of a thermally responsive material using only a single input: electric current. We have previously demonstrated variable stiffness using a thermoplastic in a fabric-based system [4] and the integration of shape memory alloy (SMA) into fabric to form compliant and actuating planar structures [1]. This letter combines these two bodies of work into an integrated, active, variable stiffness material that demonstrates performance as a multifunctional active variable stiffness fabric (AVS fabric). By combining both actuation and variable stiffness functions, the AVS fabric can change the position of a soft structure and hold the new position without requiring additional power. Figure 1 shows the AVS fiber sewn into muslin fabric (an inextensible cotton textile) to form an AVS fabric.

This letter contributes the following innovations: (1) integrated actuation and variable stiffness functions in a single fiber, enabled by a novel room-temperature manufacturing technique that avoids activation of the thermally responsive materials during processing, (2) coupled and un-coupled actuation and variable stiffness, achieved by tuning the thermoplastic's glass-transition temperature either higher or lower than the activation temperature of the SMA actuator, and (3) multifunctional fabrics with integrated active variable stiffness fibers. The integrated fabric demonstrates both actuation and variable stiffness on-demand. The fabric acts as a connecting medium where multiple fibers can be integrated and activated in parallel, thereby increasing overall lifting and holding capacity. Figure 1(a)–(b) demonstrates the AVS fabric lifting a 200 g mass and holding it suspended even after power has been shut off to the system. The serpentine pattern of the stiffness element enables the fabric to support the 200 g mass suspended between two blocks when not activated (Figure 1(c)). After being softened, the fabric is then allowed to deform under the weight (Figure 1(d)).

## II. PREVIOUS WORK

Variable stiffness actuators for soft machines have taken two approaches: system-level and material-level. System-level variable stiffness actuators contain elastic and/or damping elements or employ control algorithms to tune the stiffness and impedance of the device [5]–[11]. Variable stiffness actuators may also derive their stiffness control at the material level. For example, the McKibben actuator is a widely-used soft pneumatic actuator, consisting of a braided mesh that shortens in length and increases in stiffness as it is inflated with air (the stiffness and actuation are coupled) [12], [13]. Similarly, changes in both volume and rigidity have been demonstrated by swelling of polymer gels [14]. Wang, et al. developed a composite system using SMA wire actuators and a low-melting point fusible alloy as a variable stiffness component, then encapsulated both in a silicone elastomer [15].

Multifunctional fibers have been developed by researchers to duplicate the tensile strength and actuation capabilities of natural muscle fibers. Approaches include the use of carbon nanotubes to create a conductive, strong fiber [16]–[18], with a disadvantage of small displacements (less than 5%), micron sizing, and an inability to maintain a structural shape. Other recent work created fibers using polymer structures [19], but these fibers also only provide actuation and tensile strength without structural rigidity.

In the broader community of robotic fabrics, shape memory alloy wires are a common actuator choice due to ease of integration by stitching [1], felting [2], weaving [20], [21], and other fixture methods [3]. Previously demonstrated active fabrics have been used in robotic applications [1], kinetic and technical garments [2], [22], and self-deploying structures [20], [23]. Our previous work demonstrated variable stiffness fibers integrated into fabrics to distribute stiffness control over a surface [4]. These fibers leveraged the glassy-rubbery transition in thermoplastics for variable stiffness function.

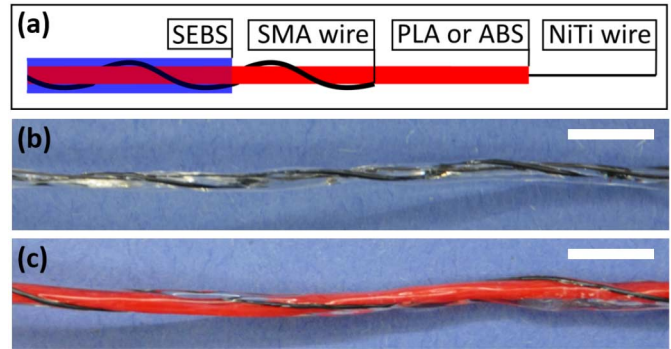


Fig. 2. Active variable stiffness fibers. (a) Diagram of the composition of an AVS fiber. (b) PLA-based AVS fiber (the PLA core and the SEBS coating are both transparent). (c) ABS-based AVS fiber. Scale bars are 1 cm.

## III. MATERIALS

The active variable stiffness (AVS) fibers were composed of an actuating shape-memory alloy (SMA) wire and a variable stiffness (VS) fiber, bound together with a polymer rubber as seen in Figure 2. The SMA wire actuator, composed of a nickel-titanium (NiTi) alloy (Dynalloy, 0.508 mm dia.), changes shape to return to a programmed helical coil when heated above its activation temperature (70 °C - 75 °C). The VS fibers were composed of a heating element coated with a film of thermoplastic that changes stiffness in response to temperature. Our previous work utilized unprogrammed NiTi wire (Dynalloy, 0.254 mm dia.) encased in a thin coating of polylactic acid (PLA) (Open Source Printing, LLC) [4]. Here, we built on this work and also introduced acrylonitrile butadiene styrene (ABS) (MakerBot Industries, LLC) as a variable stiffness coating. Both types of VS fibers reduced in stiffness when the thermoplastic was heated above its glass-transition temperature ( $T_g$ ): 55 °C - 65 °C for the PLA [4], and 105 °C for the ABS (manufacturer specified). Though ABS has a lower stiffness than PLA, we included it in this study because it has a higher  $T_g$  than the SMA transition temperature. This allows us to couple and decouple the variable stiffness effect from the SMA actuation, using the PLA and ABS as the stiffening material, respectively. The SMA actuator and VS fibers were bound together by encapsulating them with polystyrene-*block*-poly(ethylene-*ran*-butylene)-*block*-polystyrene (SEBS) (Sigma-Aldrich,  $M_w = 89,000$ ), a polymer rubber that withstands the operating temperatures of the fibers and remains rubbery even below room temperature.

We note here that although the NiTi heating wire used in the VS fibers can also exhibit the shape-memory effect if properly programmed, in our work it was used purely for its efficacy as a Joule heater. In the following discussions, the heating wire in the VS fibers will be referred to as NiTi wire; the SMA actuator will be referred to as SMA wire.

## IV. MANUFACTURING METHODS

### A. Variable Stiffness Fibers

In this work, we manufactured two varieties of AVS fibers: ABS-based and PLA-based. Drawing upon our previous work,

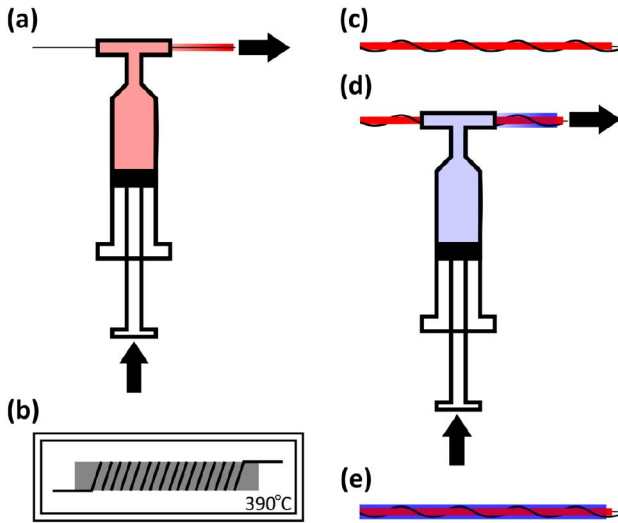


Fig. 3. Manufacturing ABS-based active variable stiffness fibers. (a) Coating ABS solution onto a heating NiTi wire for variable stiffness fiber. (b) Programming active SMA wire into a helical coil in a 390 °C oven. (c) Twisting the programmed SMA wire onto the variable stiffness fiber. (d) Encapsulating the twisted wires with SEBS. (e) Completed AVS fiber.

PLA-based variable stiffness fibers are manufactured by drawing 0.254 mm diameter NiTi wire through melted PLA thermoplastic as described by Chenal, et al. [4]. Our resulting fiber diameter was  $1.50 \pm 0.28$  mm (95% confidence).

In order to process the ABS, an amorphous polymer with no true melting point, we developed a solvent-based approach to manufacture the VS fibers at room temperature (25 °C). ABS filament (1.75 mm dia.) was cut into approximately 1 cm long pellets and then placed in a solvent (2-butanone, Sigma-Aldrich) at a 50% polymer (by weight) concentration. The mixture homogenized over a 12hr period, and was then transferred into a syringe tipped with a T-junction (4 mm inner dia.). The solution was allowed to degas for 4hrs. To coat the wire, the NiTi wire was fed through the T-junction, as shown in Figure 3(a), at a constant rate of approximately 30 cm/min. Simultaneously, pressure was applied to the syringe to ensure the T-junction was full of the ABS mixture. At this rate of pull, the resulting thickness of the variable stiffness fiber was  $2.08 \pm 0.80$ mm (95% confidence).

### B. SMA Actuator

The SMA actuator was programmed through the following series of steps. The wire was coiling tightly onto a 9.525 mm diameter shaft (Figure 3(b)) as tension was applied to the wire. The wire was then secured onto the shaft using two collars. The shaft was then placed in an oven at 390 °C for 10min and then quenched and dried [24]. This cycle was repeated 10 times to ensure shape fixity.

### C. Integration into AVS Fiber

After the coating on the VS fiber solidified either by cooling or solvent evaporation, the SMA wire and VS fiber were twisted around each other in the same direction as the SMA's

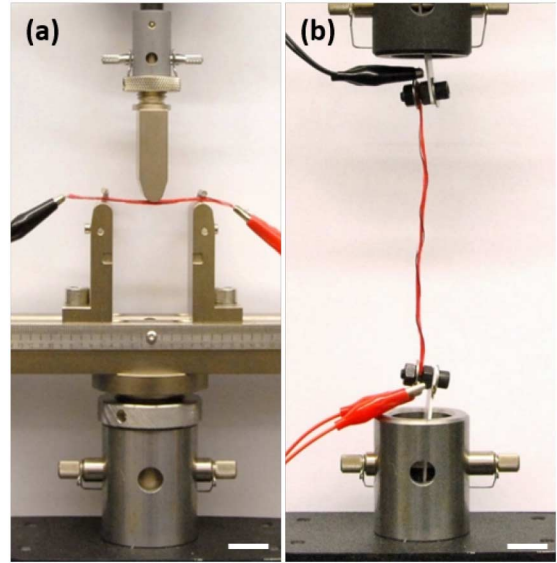


Fig. 4. Setup for characterization of AVS fibers. (a) Stiffness characterization using a 3-point bending setup. (b) Force and load characterization setup. Scale bars are 2 cm.

programming coil to prevent internal torsion, as demonstrated in Figure 3(c). This twist had a pitch of approximately 0.25 (ABS) and 0.4 (PLA) rotations per cm, influenced by the diameter of the VS fiber. The low-pitch twist bound the SMA wire and the VS fiber with a slight mechanical connection in anticipation of the next processing step. The twisted pair was then passed through a T-junction filled with a polymer solution (Figure 3(d)) composed of SEBS polymer and toluene (30% polymer, by weight), prepared in a manner similar to the ABS 2-butanone solution, to bond the two components together. After the toluene evaporated from the SEBS coating, the AVS fiber was complete (Figure 3(e)). The final diameter of the ABS-based AVS fiber was  $2.78 \pm 0.20$ mm (95% confidence); the final diameter of the PLA-based AVS fiber was  $2.04 \pm 0.18$ mm (95% confidence). Because of the VS fibers' small diameter, the twisted SMA can be approximated as linear along the length of the VS fiber, allowing the SMA to deform without interference when activated.

## V. CHARACTERIZATION

### A. Stiffness Characterization

We characterized the AVS fibers with the thermoplastic in the inactive (stiff, glassy) state and active (soft, rubbery) state. We did this with a 3-point bending test using an Instron 3345 as seen in Figure 4(a). The distance between supports was 5 cm and the nose radius was 5 mm. In our tests, strain was applied at a rate of 0.01(mm/mm)/min. The glassy state tests were performed at room temperature (25 °C). To achieve the rubbery state, the VS fibers, contained within the AVS fibers, were activated for 5s at  $I = 0.75A$  before the start of the test to transition the thermoplastic into the rubbery state. Each fiber specimen was tested three times in both glassy and rubbery states.

The bending modulus, calculated as the ratio of the bending stress to the bending strain, was determined for three specimens of each type of AVS fiber. The 3-point bending test

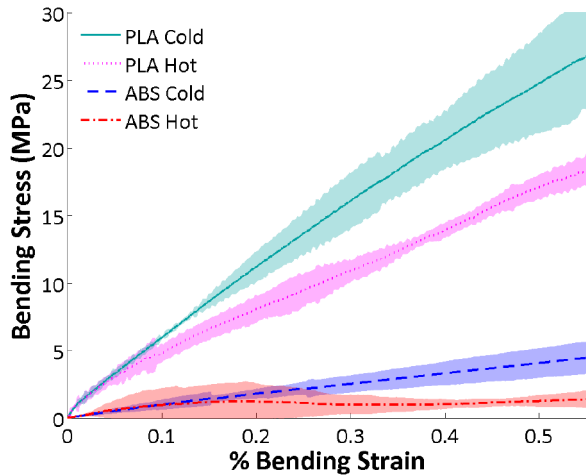


Fig. 5. Stress-strain plot for two AVS fibers in a 3-point bending setup. A PLA-based and an ABS-based AVS fiber were tested repeatedly in stiff (cold) and softened (hot) states. The shaded area around each average line represents a 95% confidence interval.

TABLE I  
BENDING MODULUS OF ABS- AND PLA-BASED AVS FIBERS WITH THE STIFFENING THERMOPLASTIC HEATED ( $>T_G$ ) AND COOLED ( $25^\circ\text{C}$ ).  
 $\pm$  VALUE IS 95% CONFIDENCE ON MEAN

		Bending modulus (GPa)	
		Cold VS fiber	Hot VS fiber
ABS	Specimen 1	$0.89 \pm 0.12$	$0.34 \pm 0.24$
	Specimen 2	$0.72 \pm 0.18$	$0.17 \pm 0.25$
	Specimen 3	$0.57 \pm 0.16$	$0.17 \pm 0.20$
	Average Modulus	$0.73 \pm 0.15$	$0.23 \pm 0.23$
PLA	Specimen 1	$3.91 \pm 2.60$	$0.42 \pm 1.31$
	Specimen 2	$4.73 \pm 3.09$	$0.82 \pm 0.26$
	Specimen 3	$5.12 \pm 3.70$	$2.52 \pm 1.09$
	Average Modulus	$4.59 \pm 3.13$	$1.25 \pm 0.89$

provided a set of stress-strain data points that follow a linear trend in the elastic range of the material (Figure 5). We fit a straight line to each data set to obtain the bending modulus from the slope of fitted line, given in Table I. This table shows the bending modulus fluctuated from one specimen to another. We attributed the variation between the values from each specimen to two sources: manufacturing inconsistency and geometric anisotropy. Manufacturing inconsistency refers to variation in the thermoplastic and SEBS coating thicknesses, which resulted in variance in the cross-sectional geometry of both the VS fibers and the AVS fibers. The geometric anisotropy of the AVS fibers arises from the change in position of the SMA wire relative to the loading direction as the fiber is rotated during the 3-point bending test. The maximum stiffness configuration occurs when the loading direction is aligned with the axis passing through the center of both the VS fiber and SMA, and the minimum stiffness configuration occurs when the loading direction is orthogonal to this axis. To ensure that the measured values are within reason, we performed a stiffness analysis of the cross-section by integrating the second moment of area and elastic modulus to determine the overall bending modulus of the AVS fibers in their stiffened state. By considering the upper and lower extremes for both coating

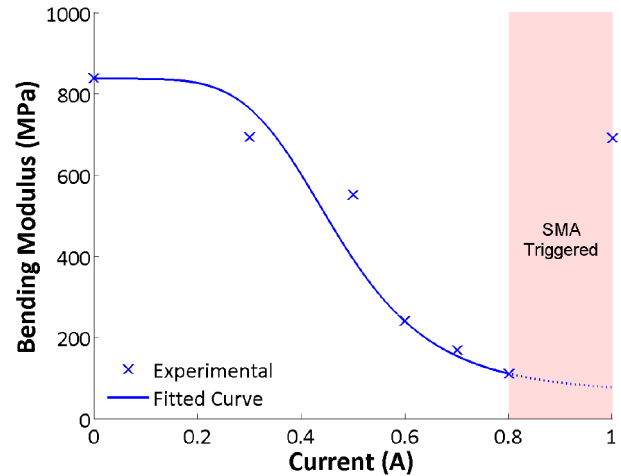


Fig. 6. Stiffness characterization plot for a single ABS-based AVS fiber softened with various currents. At high currents, the SMA actuator begins to activate during the stiffness test resulting in an increased modulus.

thicknesses and geometric anisotropy, we calculated possible modulus ranges as 0.453-4.80GPa and 2.11-7.70GPa for the ABS-based and PLA-based fibers, respectively. These ranges include the values that we measured (Table I), confirming that the spread of the experimental values is within reason.

The bending modulus was also determined as a function of current for a single representative ABS-based AVS fiber specimen (Figure 6). We varied the current from 0A to 1A, focusing on the currents near the transition from the stiff to soft state. A sigmoidal curve fit to the experimental data follows the trend expected of a thermoplastic's modulus going through its  $T_g$  [25]. However, the trend breaks at the higher currents (represented by the 1A data point) when the heated VS fiber is hot enough to trigger activation of the adjacent SMA actuator, transitioning the SMA from its flexible martensite phase into a stiff austenite phase, thereby increasing the general bending modulus of the AVS fiber. This curve provided us with a range of currents to use that would soften the ABS-based AVS fiber. The PLA-based AVS fibers were not characterized in this work, as a similar analysis appears in previous work done by Chenal, et al. [4].

The average modulus values presented in Table I shows that the ABS-based fibers are softer than the PLA fibers both when stiffened and softened. To determine how the stiffnesses of the fibers affect actuation, we subsequently performed force tests on the fibers.

### B. Force and Load Characterization

To characterize the force produced by the AVS fibers, 10 cm long AVS fiber segments were clamped in an Instron 3345 fitted with a 50N load cell (Figure 4(b)). Throughout the test, the specimens were held in tension at a fixed length to measure the force produced by the isometrically actuating SMA when the VS fiber was both stiff and softened.

In contrast to the stiffness tests, only the ABS-based AVS fibers were tested for force in both their stiffened and soft state. The PLA-based fibers were tested only in their soft state,

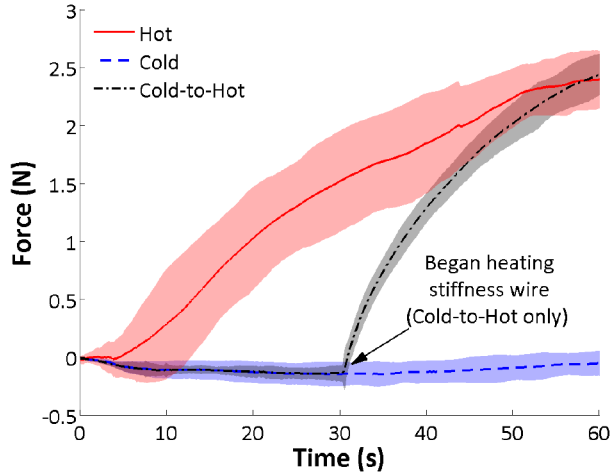


Fig. 7. Plot of force produced by an ABS-based AVS fiber. Hot: VS fiber was softened before SMA actuation. Cold: VS fiber was not softened before SMA actuation. Cold-to-Hot: VS fiber was softened 30s after the SMA was actuated. The shaded area around each average line represents a 95% confidence interval.

TABLE II

FORCE PRODUCED BY THE SMA ACTUATOR PORTION OF ABS- AND PLA-BASED AVS FIBERS IN THE SOFTENED AND STIFFENED STATE.  $\pm$  VALUE IS 95% CONFIDENCE ON MEAN

		Force (N)
ABS-based fiber	Soft state	$2.25 \pm 0.17$
	Stiff state	$-0.09 \pm 0.22$
PLA-based fiber	Soft state	$1.04 \pm 0.30$
	Stiff state	N/A

because the PLA stiffness cannot be decoupled from the SMA actuation. Since the  $T_g$  of PLA is below the activation temperature of SMA, when the SMA is powered the PLA will soften regardless of whether or not the VS fiber is powered. This effect does not occur in the ABS-based fibers because the  $T_g$  of ABS is above the activation temperature of SMA—only overheating the SMA will cause the ABS to transition into the rubbery state.

We averaged the tests from multiple segments of the ABS-based AVS fiber (Table II). When the ABS was softened, the SMA was able to produce  $2.25 \pm 0.17$ N of actuation force. In contrast, when the ABS was stiff, the testing apparatus was unable to detect any pulling forces from the SMA wire. The negative force values result from the hot SMA reducing the whole fiber’s modulus slightly. This test demonstrates that the ABS-based AVS fiber will maintain its position when the VS fiber is inactive, even when the SMA is powered. The results also show that the ABS-based AVS fibers produce higher forces compared to the PLA-based AVS fibers. This is likely due to a both the PLA having a higher bending modulus than ABS in its soft state (Table I) and the soft ABS adding heat to the SMA wire.

In Figure 7, we plotted the data from a single ABS-based AVS fiber showing the force being generated from the active SMA wire over time for 60s. The fiber was subjected to 3 operating conditions: 1) actuation of the SMA without softening the ABS, 2) actuation of the SMA after softening the ABS, and 3) actuation of the SMA for 30s prior to softening the ABS. These conditions are shown in Figure 7 as “Cold”,

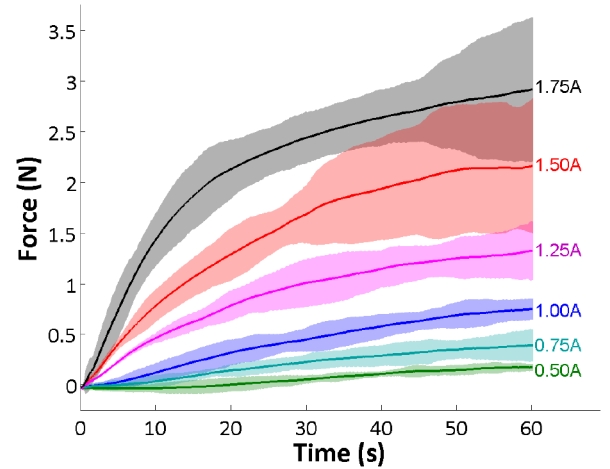


Fig. 8. Plot of force produced by an ABS-based AVS fiber as a function of applied current. The VS fiber was softened prior to the start of each run. The currents applied ranged from 0.5A to 1.75A in increments of 0.25A. The shaded area around each average line represents a 95% confidence interval.

“Hot”, and “Cold-to-Hot”. The plot clearly shows that the fiber follows the zero-force trend when the fiber is stiff, but once the fiber is softened, the actuating SMA is able to produce force. This demonstrates complete decoupling of the actuation and stiffening components in the ABS-based AVS fibers.

We further characterized a single ABS-based AVS fiber for the force produced as a function of current applied (Figure 8). For all of these experiments, the VS fiber was softened prior to actuating the SMA, identical to the “Hot” tests shown in Figure 7. We measured the amount of force produced by the fiber over 60s of applied current across a range from 0.5A to 1.75A. As expected, increasing the input current results in increased output force, showing that the incorporation of the SMA actuator in an AVS fiber does not change the SMA actuation behavior [24].

In addition to the force generation experiments, we also characterized the load capacity of the fibers and SMA wire in their stiffened, coiled shape. The fibers and wire were first actuated (without load) then cooled into a fully contracted coil. This stiffened coil was then placed in the same Instron setup shown in Figure 4(b). We applied a constant linear displacement of 10 mm/min to the coil and measured the resulting load. The resulting load-extension curve indicated that the coils behaved as linear springs with spring constants of  $3.85 \pm 2.91$  N/m for the SMA wire,  $22.2 \pm 6.28$ N/m for the PLA-based AVS fibers, and  $51.8 \pm 14.8$ N/m for the ABS-based AVS fibers (95% confidence).

## VI. APPLICATIONS

### A. Single-Fiber Active Lifting and Passive Holding

To demonstrate the “move and hold” potential of AVS fiber, we lifted a 47 g mass with the AVS fiber and then removed power to the system, allowing the fiber to passively hold the weight. As shown in Figure 9, we compared a programmed SMA actuation wire with the PLA-based and ABS-based AVS fibers. The bare SMA actuator wire is identical to the actuation

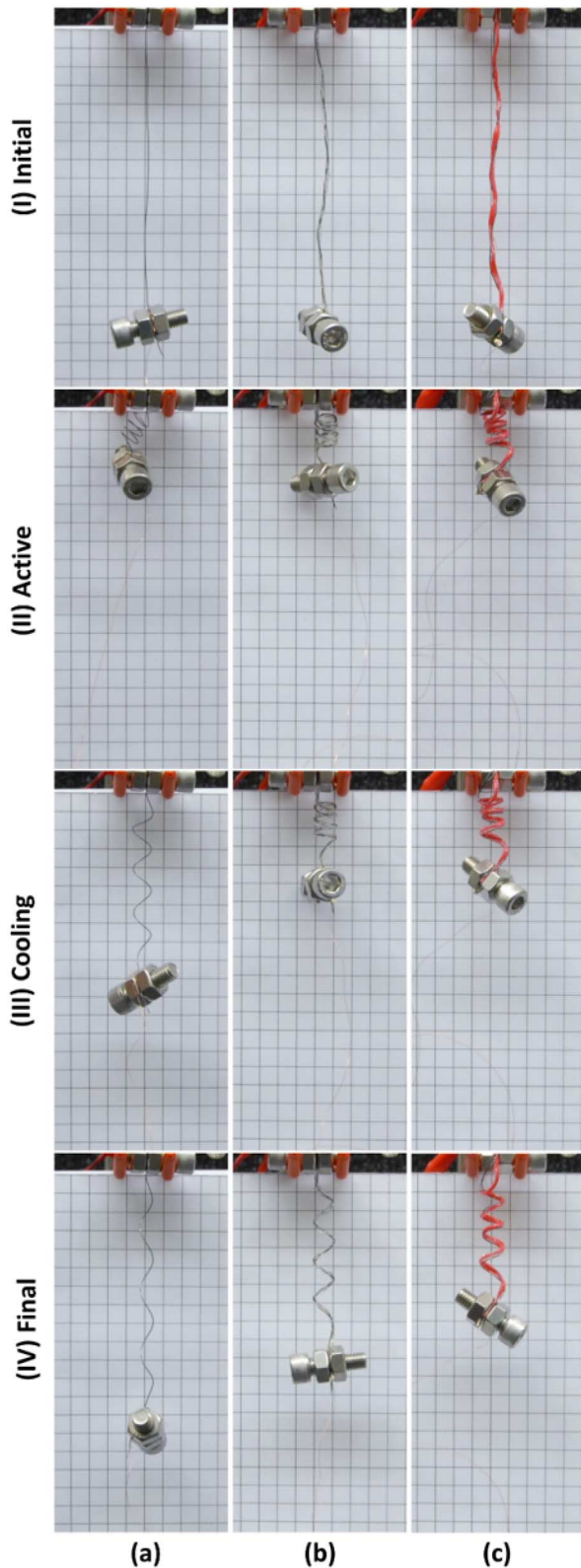


Fig. 9. Comparison of an actuation cycle of (a) an SMA wire, (b) a PLA-based AVS fiber, and (c) an ABS-based AVS fiber. The top of the fiber is fixed and a 47 g mass is attached to the hanging end of the fiber. The mass acts as an electrode, with a small copper wire attached to it. From top to bottom: (I) the fiber is not actuated, (II) the fiber is softened and fully actuated, (III) all power is turned off to the fiber, and it is allowed to cool for 15s, (IV) the fiber is completely cooled. For scale, each square is 1 cm<sup>2</sup>.

wire in the AVS fibers. To set up the test, we clamped a 15 cm segment of the fiber to a support, then hung a mass from the free end of the fiber, applying a downward force. The bottom leads of the fiber were attached to the weight making it a common ground for the fiber. A small copper wire of negligible mass (0.2 g) was attached to the weight and traveled with the weight to maintain electrical contact.

For each test, after hanging the fiber, the NiTi wire was heated briefly to soften the variable stiffness thermoplastic (Figure 9(I)). Current was then applied to the SMA actuator to lift the weight. Both the VS fiber and SMA wire were powered until the SMA actuator achieved maximal displacement (Figure 9(II)). At this point, all power to the fibers was shut off, and the entire AVS fiber was allowed to cool. The AVS fiber relaxation was recorded 15 seconds after the power was shut off (Figure 9(III)) and 5 minutes later (Figure 9(IV)) when the fibers had completely cooled. The SMA wire was tested using this same procedure, without the initial step of heating up a variable stiffness fiber prior to actuation.

Figure 9 presents the results of this test. The bare SMA wire lifted the bolt higher than the AVS fibers by 1 cm, but once the power was disconnected the weight dropped 11 cm (85%) (Figure 9(a)). The PLA-coated AVS fiber lifted the bolt 12 cm, but lost 7 cm (58%) of this initial displacement during cooling (Figure 9(b)). In comparison, the ABS-based fiber lifted the bolt up 12 cm and then, upon cooling, only lost 4 cm (33%) of its actuation height (Figure 9(c)).

According to the previously calculated spring constants, the displacement (the distance between actuation height and final height) for each fiber type was predicted as 11 cm, 2.08 cm and 0.89 cm for the SMA wire, PLA-based, and ABS-based fibers, respectively. While the actual displacement of the SMA wire was consistent with the predicted displacement, the actual displacement of the AVS fibers was greater than predicted. We attribute this discrepancy to the cooling and re-stiffening period of the thermoplastic. As the AVS fibers cool down (Figure 9(III)), the ABS is able to drop below its  $T_g$  and stiffen even while the SMA is still at its activation temperature. In contrast, the PLA remains soft while the SMA cools below its activation temperature. With no lifting force, the weight can stretch out the PLA-based fiber more than the ABS-based fiber. This explains why both fibers dropped more than their spring constants predicted, as well as why the PLA-based fiber dropped an additional 5 cm when the ABS-based fiber dropped only an additional 3 cm.

It is important to note that the bare SMA wire actuated significantly faster than the other two AVS fibers. Though we did not record the data precisely, the overall activation time for the SMA wire was 20-30s shorter than the tests for the AVS fibers (about 60-70s).

### B. AVS Fabric for Conformable Robotic Skins

The second test demonstrates the potential of these AVS fibers to be used in robotic fabric. We sewed a long ABS-based AVS fiber to a strip of cotton fabric, creating a fabric capable

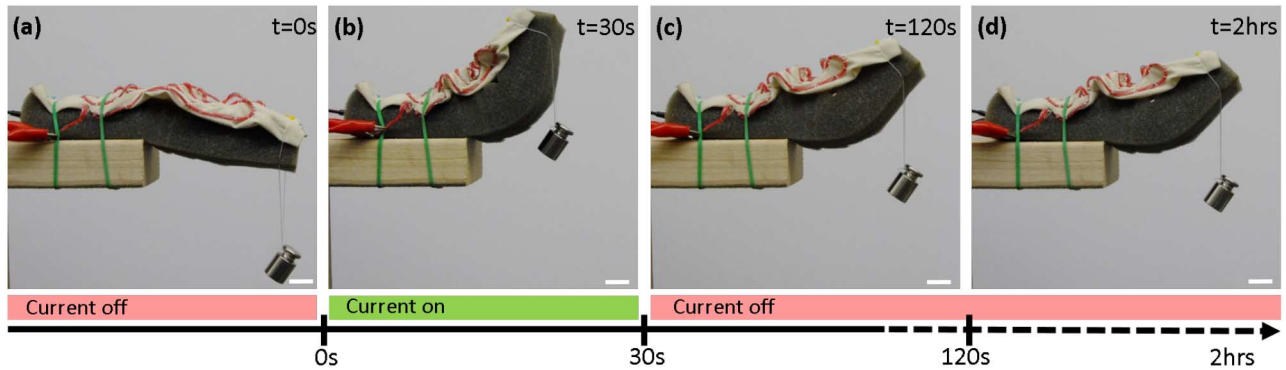


Fig. 10. AVS fabric attached to a cantilevered foam block to create a soft robotic lifting arm structure. One end of the foam block is fixed; the other end is free and supports a 50 g mass. (a) AVS fabric is stiff, (b) AVS fabric is softened and fully actuated, (c) AVS fabric is stiff and cooling, and (d) Robotic arm structure sustaining mass for extended period of time with no additional power input. Scale bars are 2 cm.

of manipulating objects from their surface. The AVS fiber adds both structure and function the fabric, giving the fabric the ability to mechanically manipulate objects (Figure 10). Figure 1(a)–(b) shows the AVS fabric used in this demonstration in both a flattened and actuated state. The holding capability of the ABS-based fibers from the first demonstration encouraged us to choose these fibers over the PLA-based fibers in our final demonstration. We stitched the AVS fiber at 2 cm intervals in a serpentine pattern consisting of six lines. This stitch length adequately secured the AVS fibers to the fabric without constricting the AVS fiber deformation during actuation.

We attached the AVS fabric to the top of a foam block as shown in Figure 10(a) to simulate a soft robotic arm. The foam block was fixed in a cantilever position with a 50 g mass suspended from the free end. In Figure 10(a), the fabric is stiff with the mass causing the foam block to sag. After softening the VS fiber with 0.75A of current and actuating the programmed SMA for 30s at 1.5A, the fully actuated state of the AVS fabric is attained (Figure 10(b)), lifting the mass 10 cm. Immediately after full actuation, power was disconnected to the fiber and the AVS fabric was left to cool. While the AVS fabric was cooling to a glassy, stiffened state, the spring-force of the curled foam block and the weight of the 50 g mass pulled the foam arm partially down from the fully actuated position (Figure 10(c)). The soft robotic arm structure then sustained the weight 5.75 cm higher than its original position with no additional energy input, for 2hrs. Figure 10(d) shows the structure holding the weight, with the weight only dropping an additional 0.75 cm from the 2 minute mark in Figure 10(c). This small drop in position can be attributed both to creep in the polymer and the AVS fabric not having fully cooled at the 2 minute mark.

## VII. CONCLUSION AND FUTURE WORK

In this work, we have demonstrated active variable stiffness fibers for use in conformable robotic applications. The active variable stiffness fibers are comprised of two functional elements intertwined: a variable stiffness fiber and an actuating shape memory alloy wire. Both fibers are activated by thermal energy generated by Joule heating. The active variable stiffness

fibers can actuate and sustain displacements even after power has been disconnected from the system.

We introduced active variable stiffness fibers using two different thermoplastics: PLA and ABS. Because the  $T_g$  of PLA is below the SMA activation temperature, the variable stiffness effect is coupled to SMA actuation. In contrast, the  $T_g$  of ABS is higher than the SMA activation temperature, and thus the variable stiffness and actuation are decoupled. The fibers were characterized for their change in stiffness and for force production. We studied the behavior of individual AVS fibers in performing a “move-and-hold” operation, demonstrating an improved holding capacity in the ABS-based due to the decoupled stiffening and actuation. The ABS-based AVS fibers were used to manufacture an active variable stiffness fabric by stitching the fibers onto cotton fabric. By attaching the planar AVS fabric to a soft foam block, motion and stiffness control was imparted upon the foam. Actuation of the fabric caused the foam block to bend and lift a mass, then proceed to hold the deformation without continuous actuation via stiffening of the fabric. This demonstrated that the 1D capabilities of multifunctional fibers can be extended to 2D surfaces and 3D structures.

Future work will focus on optimization of the manufacturing process and further characterization of the fibers. An improved manufacturing framework would increase control over the cross-sectional geometry of the fibers, allowing for greater customizability and uniformity of the fibers’ function. Full characterization of the stiffness and force production would enable a better understanding of the behaviors and functional coupling of the fibers. Additionally, future work may explore the use of other materials, such as alternatives to the stiffening agent and encapsulation polymer, as it is possible to tune the fibers precisely to structural and/or performance requirements. Additionally, a parametric study to determine the effect of different diameters of wire, thickness of polymer coatings, and twisting pitch may contribute to future design optimization. Future work will also explore the effect of different or more complex sewing patterns on the performance of AVS fabrics, as well as the addition of sensing elements for proprioceptive feedback, enabling closed-loop control of a robotic fabric.

## ACKNOWLEDGMENT

The authors would like to thank Edward White for assistance with manufacturing and Prof. Kendra Erk (Purdue University) for assistance with the materials selection. Any opinion, findings, and conclusions or recommendations expressed in this material are those of the authors and do not necessarily reflect the views of the National Aeronautics and Space Administration or the National Science Foundation.

## REFERENCES

- [1] M. Yuen, A. Cherian, J. C. Case, J. Seipel, and R. K. Kramer, "Conformable actuation and sensing with robotic fabric," in *Proc. IEEE/RSJ Int. Conf. Intell. Robots Syst. (IROS'14)*, 2014, pp. 580–586.
- [2] J. Berzowska and M. Coelho, "Kukkia and vilkas: Kinetic electronic garments," in *Proc. IEEE Int. Symp. Wearable Comput.*, 2005, pp. 82–85.
- [3] B. Holschuh and D. Newman, "Two-spring model for active compression textiles with integrated NiTi coil actuators," *Smart Mater. Struct.*, vol. 24, no. 3, p. 035011, Mar. 2015.
- [4] T. Chenal, J. Case, J. Paik, and R. Kramer, "Variable stiffness fabrics with embedded shape memory materials for wearable applications," in *Proc. IEEE/RSJ Int. Conf. Intell. Robots Syst. (IROS'14)*, Sep. 2014, pp. 2827–2831.
- [5] B. Vanderborght *et al.*, "Variable impedance actuators: A review," *Robot. Auton. Syst.*, vol. 61, no. 12, pp. 1601–1614, Dec. 2013.
- [6] A. Bicchi, G. Tonietti, M. Bavaro, and M. Piccigallo, "Variable stiffness actuators for fast and safe motion control," in *Proc. 11th Int. Symp. Robot. Res.*, 2005, pp. 527–536.
- [7] B.-S. Kim and J.-B. Song, "Hybrid dual actuator unit: A design of a variable stiffness actuator based on an adjustable moment arm mechanism," in *Proc. IEEE Int. Conf. Robot. Autom. (ICRA)*, May 2010, pp. 1655–1660.
- [8] S. Wolf and G. Hirzinger, "A new variable stiffness design: Matching requirements of the next robot generation," in *Proc. Int. Conf. Robot. Autom. (ICRA'08)*, May 2008, pp. 1741–1746.
- [9] C. E. English and D. Russell, "Mechanics and stiffness limitations of a variable stiffness actuator for use in prosthetic limbs," *Mech. Mach. Theory*, vol. 34, no. 1, pp. 7–25, Jan. 1999.
- [10] G. Tonietti, R. Schiavi, and A. Bicchi, "Design and control of a variable stiffness actuator for safe and fast physical human/robot interaction," in *Proc. IEEE Int. Conf. Robot. Autom. (ICRA'05)*, Apr. 2005, pp. 526–531.
- [11] L. Visser, R. Carloni, and S. Stramigioli, "Energy-efficient variable stiffness actuators," *IEEE Trans. Robot.*, vol. 27, no. 5, pp. 865–875, Oct. 2011.
- [12] C.-P. Chou and B. Hannaford, "Static and dynamic characteristics of McKibben pneumatic artificial muscles," in *Proc. IEEE Int. Conf. Robot. Autom.*, 1994, pp. 281–286.
- [13] Y. Shan *et al.*, "Variable stiffness structures utilizing fluidic flexible matrix composites," *J. Intell. Mater. Syst. Struct.*, vol. 20, no. 4, pp. 443–456, Mar. 2009.
- [14] C. Santulli, S. I. Patel, G. Jeronimidis, F. J. Davis, and G. R. Mitchell, "Development of smart variable stiffness actuators using polymer hydrogels," *Smart Mater. Struct.*, vol. 14, no. 2, p. 434, Apr. 2005.
- [15] W. Wang, H. Rodrigue, and S.-H. Ahn, "Smart soft composite actuator with shape retention capability using embedded fusible alloy structures," *Compos. B, Eng.*, vol. 78, pp. 507–514, Sep. 2015.
- [16] M. D. Lima *et al.*, "Electrically, chemically, and photonically powered torsional and tensile actuation of hybrid carbon nanotube yarn muscles," *Science*, vol. 338, no. 6109, pp. 928–932, Nov. 2012.
- [17] T. Mirfakhrai *et al.*, "Electrochemical actuation of carbon nanotube yarns," *Smart Mater. Struct.*, vol. 16, no. 2, p. S243, Apr. 2007.
- [18] J. Foroughi *et al.*, "Torsional carbon nanotube artificial muscles," *Science*, vol. 334, no. 6055, pp. 494–497, Oct. 2011.
- [19] C. S. Haines *et al.*, "Artificial muscles from fishing line and sewing thread," *Science*, vol. 343, no. 6173, pp. 868–872, Feb. 2014.
- [20] G. K. Stylios and T. Wan, "Shape memory training for smart fabrics," *Trans. Inst. Meas. Control*, vol. 29, nos. 3–4, pp. 321–336, Aug. 2007.
- [21] S.-I. Vasile, K. E. Grabowska, I. L. Ciesielska-Wrobel, and J. Ghitaiga, "Analysis of hybrid woven fabrics with shape memory alloys wires embedded," *Fibres Text. East. Eur.*, vol. 18, no. 1, pp. 64–69, 2010.
- [22] Y. Y. F. C. Vili, "Investigating smart textiles based on shape memory materials," *Text. Res. J.*, vol. 77, no. 5, pp. 290–300, May 2007.
- [23] J. Hu, *Adaptive and Functional Polymers, Textiles and Their Applications*. Singapore: World Scientific, 2010.
- [24] S. Seok, C. D. Onal, K.-J. Cho, R. J. Wood, D. Rus, and S. Kim, "Meshworm: A peristaltic soft robot with antagonistic nickel titanium coil actuators," *IEEE/ASME Trans. Mechatron.*, vol. 18, no. 5, pp. 1485–1497, Oct. 2013.
- [25] N. G. McCrum, C. P. Buckley, and C. B. Bucknall, *Principles of Polymer Engineering*. London, U.K.: Oxford Univ. Press, Jan. 1997.